Photoreactivity of Polymers with Regioisomeric Cinnamate Side Chains and Their Ability To Regulate Liquid Crystal Alignment†

**Kunihiro Ichimura,* Yasuhiro Akita, Haruhisa Akiyama,
Kazuaki Kudo, and Yuko Hayashi**

*Research Laboratory of Resources Utilization, Tokyo Institute of Technology,
4259 Nagatsuta, Midori-ku, Yokohama 226, Japan*

Received August 13, 1996; Revised Manuscript Received December 4, 1996⊗

ABSTRACT: Photoproduct distribution in films of cinnamate polymers was analyzed to reveal the contribution of both photoisomerization and photodimerization to LC alignment photoregulation. A polymethacrylate with *o*-cinnamate side chains displayed preferential formation of *Z*-isomer while the dimerization takes place more favorably for other polymers including poly(vinyl cinnamate). On the basis of the relationship between photoproduct distribution and liquid crystal photoalignment and on the reversibility of the photoinduced reorientation of a liquid crystal, it was concluded that the photoalignment results from the polarization photoisomerization of cinnamate residues in the same manner as that of photochromic moieties like azobenzenes, whereas the (2 + 2) photodimerization plays a role in enhancing the thermal stability of the homogeneous photoalignment.

Introduction

Conventional negative-working photoresists, poly(vinyl cinnamates) (PVCi's), played a prominent and leading role in science and technology of photopolymers since their invention 4 decades ago.[1] Their photofunctionality arises from (2 + 2) photodimerization leading to insolubilization due to the formation of cross-linking bonds. Two decades after the invention, it was reported that the photoinduced chemical transformation of photo-cross-linkable pVCi shows a novel optical property. Owing to the emergence of birefringence upon linearly polarized light irradiation, it exhibits polarization holography.[2,3] Recent advances in polarization photochemistry of molecular and polymeric ultrathin films leading to orientational regulation of liquid crystal molecules[4−14] has made the potential use of this type of conventional photoresists significantly more attractive. The exposure of a thin film of pVCi and its derivatives to linearly polarized UV light induces a uniaxial reorientation of a liquid crystal (LC) layer.[15−22] The surface-assisted photoalignment regulation of LCs has been attracting current interest because of the practical applicability of the rubbing-free production of LC aligning films[6,22] as well as versatile optical elements with birefringent characteristics[6,7,17] so that the elucidation of a working mechanism of the photoalignment regulation with cinnamate polymers is now urgenty required.

According to Schadt et al., the surface-settled homogeneous alignment of nematic LCs results from linearly polarized light (LPL) induced photodimerization of cinnamate moieties in polymer thin films to form cyclobutane ring systems with an azimuthally orientated order that determines the direction of LC alignment.[15] On the other hand, our systematic studies on command surfaces have revealed that the photoinduced homogeneous LC alignment is caused by polarization photochromism at uppermost surfaces of substrates as a result of repeated *E*/*Z* photoisomerization of photochromic units such as azobenzenes[8−13] and stilbenes.[14] The photochemistry of cinnamates involves two photoreactions; the (2 + 2) photodimerization and the *E*/*Z* photoisomerization (Figure 1). We have shown recently that the polarized light irradiation of sub-monolayered cinnamate moieties tethered covalently from a silica substrate surface gives a homogeneous alignment regulation and suggests that the alignment is induced by the *E*/*Z* photoisomerization of the olefinic residues, based on the effect of irradiation wavelength.[23] The purpose of this paper is to disclose that the photoreactivity of polymers having cinnamate residues is highly structure-dependent and that the homogeneous alignment of LC arises not from the photodimerization but from the LPL-induced reorientation of cinnamate side groups of polymers as a result of polarized *E*/*Z* photoisomerization.[24]

Experimental Section

Materials. Commercially available methyl cinnamate was distilled before use. Poly(vinyl cinnamate) was prepared by the esterification of poly(vinyl alcohol). Quartz plates were cleaned by sequential ultrasonical treatment for 10 min in the following fluids: acetone, concentrated HNO_3, deionized water, a saturated $NaHCO_3$ aqueous solution and deionized water. They were finally dried at 120 °C before use.

Methyl Hydroxycinnamates. Methyl (*E*)-2-hydroxy-4-methoxycinnamate (as a Typical Procedure). A benzene (10 mL) solution of 2-hydroxy-4-methoxybenzaldehyde (1.37 g, 9.00 mmol) and methyl (triphenylphosphoranylidene)-acetate (3.14 g, 9.40 mmol) was stirred for 2 h at room temperature, followed by washing with water. Conventional workup gave pale yellow crystals of methyl (*E*)-2-hydroxy-4-methoxycinnamate (mp 133−136 °C, 83%). Purification was made by column chromatography on silica gel using a 3:1 mixture of hexane and ethyl acetate as an eluent. ^{1}H-NMR ($CDCl_3$): δ (ppm) 3.70 (s, 3H, CH_3O), 3.76 (s, 3H, $COOCH_3$), 6.45 (m, 3H, CH=C*H*COO, Ar-H), 7.41 (d, 1H, Ar-H), 7.90 (d, 1H, C*H*=CHCOO). Calcd for $C_{12}H_{12}O_4$: C, 63.42; H, 5.77. Found: C, 63.98; H, 5.91.

The following were prepared in the same way:

Methyl (*E*)-2-hydroxycinnamate as colorless needles of mp 139−140 °C in 45% yield. ^{1}H-NMR ($CDCl_3$ + DMSO-d_6): δ (ppm) 3.75 (s, 3H, $COOCH_3$), 5.85 (s, 1H, OH), 6.57 (d, 1H, CH=C*H*COO, J = 16.5 Hz), 7.12 (m, 4H, Ar-H), 7.95 (d, 1H, C*H*=CHCOO, J = 16.5 Hz).

Methyl (*E*)-3-hydroxycinnamate as colorless plates of mp of 72−74 °C in 76% yield. ^{1}H-NMR ($CDCl_3$ + DMSO-d_6): δ (ppm) 3.80 (s, 3H, $COOCH_3$), 5.80 (s, 1H, OH), 6.40 (d, 1H,

---

† Command Surfaces Part 22. Part 21: Ueda, M.; Kudo, K.; Ichimura, K. *Israel J. Chem*. in press.

⊗ Abstract published in *Advance ACS Abstracts,* February 1, 1997.

S0024-9297(96)01225-9 CCC: $14.00

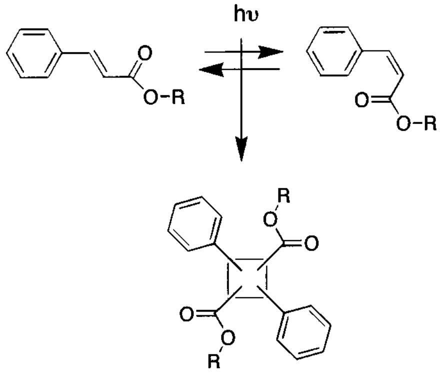

Figure 1. The photochemistry of cinnamates.

Table 1. Methyl (*E*)-Cinnamates as Low-Mass Model Compounds for Spectral Analysis

substituent	mp (°C)	λ_{max}[a] (nm)	λ_{iso}[b] (nm)	ϵ at λ_{max}[c]	
				ϵ_E	ϵ_Z
2-(2-hydroxyethoxy)-	73–74	314		1.25×10^4	9.35×10^3
4-methoxy		324		1.06×10^4	5.76×10^3
2-acetoxy	46–47	272	244	2.20×10^4	6.70×10^3
3-acetoxy	66–67	274	254	1.92×10^4	9.45×10^3
4-acetoxy	84–85	272	252	2.29×10^4	6.74×10^3
non		274	252	2.12×10^4	1.20×10^4

[a] Wavelength at the absorption maximum of *E*-isomers. [b] Wavelength at an isosbestic point during the photoisomerzation in dioxane. [c] Absorption coefficients (L mol^{-1} cm^{-1}) of *E*- and *Z*-isomers at λ_{max} of the corresponding *E*-isomer, respectively.

CH=C*H*COO, J = 16.5 Hz), 7.00 (m, 4H, Ar-H), 7.75 (d, 1H, C*H*=CHCOO, J = 16.5 Hz).

Methyl (*E*)-4-hydroxycinnamate as colorless needles of mp 129–131 °C in 77% yield. ^{1}H-NMR ($CDCl_3$ + DMSO-d_6): δ (ppm) 3.75 (s, 3H, $COOCH_3$), 6.25 (d, 1H, CH=C*H*COO, J = 16.2 Hz), 6.40 (d, 2H, Ar-H, J = 8.7 Hz), 7.30 (d, 2H, Ar-H, J = 8.7 Hz), 7.75 (d, 1H, C*H*=CHCOO, J = 16.2 Hz), 9.20 (s, 1H, OH).

Methyl (*E*)-2-(2-Hydroxyethoxy)-4-methoxycinnamate. A mixture of 1.25 g of 2-hydroxy-4-methoxybenzaldehyde, 0.83 g of potassium carbonate, and 1.25 g of 2-(2-bromoethyoxy)-tetrahydropyran in 10 mL of DMF was stirred at 65 °C for 5 h, followed by treatment with water and extraction of methyl (*E*)-4-methoxy-2-(2-tetrahydropyranylethoxy)cinnamate with ether. The product was purified by silica gel column chromatography to give a colorless oil in 84% yield. ^{1}H-NMR ($CDCl_3$): δ (ppm) 1.65 (m, 8H, CH_2), 3.55 (m, 2H, CH_2), 3.70 (s, 3H, CH_3O), 3.80 (s, 3H, $COOCH_3$), 4.15 (m, 2H, CH_2), 4,70 (s, 1H, CH_2C*H*-O), 6.50 (m, 3H, CH=C*H*COO + Ar-H), 7.40 (d, 1H, Ar-H), 7.90 (d, 1H, C*H*=CHCOO). The cinnamate was deprotected using trifluoroacetic acid to yield methyl (*E*)-4-methoxy-2-(2-hydroxyethoxy)cinnamate as colorless crystals of mp 51–53 °C in 83% yield. ^{1}H-NMR ($CDCl_3$): δ (ppm) 2.70 (s, 1H, OH), 3.75 (s, 3H, CH_3O), 3.80 (s, 3H, $COOCH_3$), 4.10 (m, 4H, CH_2), 6.50 (m, 3H, CH=C*H*COO + Ar-H), 7.40 (d, 1H, Ar-H), 7.90 (d, 1H, C*H*=CHCOO).

Methyl (*E*)-Acetoxycinnamates. They were prepared by acetylation of the corresponding hydroxycinnamates in pyridine with an excess of acetic anhydride and purified by recrystallization. Their properties are listed in Table 1.

Monomer Synthesis. Methyl (*E*)-2-(Methacryloyloxy)-4-methoxycinnamate (as a typical procedure). To a benzene solution (15 mL) of methyl (*E*)-2-hydroxy-4-methoxycinnamate (1.00 g) and triethylamine (0.50 g) was added 0.50 g of methacryloyl chloride dropwise at 65 °C to give colorless needles of the monomer of mp 90–91 °C in 81% yield. ^{1}H-NMR ($CDCl_3$): δ (ppm) 2.10 (s, 3H, CH_3), 3.77 (s, 3H, CH_3O), 3.82 (s, 3H, $COOCH_3$), 5.80 (d, 1H, C=CH), 6.30 (d, 1H, CH=C*H*COO, J = 15.3 Hz), 6.40 (d, 1H, C=CH), 6.70 (m, 2H, Ar-H), 7.60 (d, 1H, Ar-H), 7.90 (d, 1H, C*H*=CHCOO, J = 15.3 Hz). Calcd for $C_{16}H_{16}O_5$: C, 65.21; H, 5.84. Found: C, 65.07; H, 5.87.

Table 2. Characteristics of Cinnamate Polymers

polymer	copolym ratio cinnamate:MMA	M_w (10^{-4})	M_w/M_n	T_g (°C)	yield (%)
pVCi		27.3	1.9	78	40[a]
pMC1-*o*-Ci	1:0	3.6	2.1	82	56
pMC1-*o*-Ci (1:6)	1:5.8	19.5	4.5	84	55
pMC1-*o*-Ci (1:27)	1:27.2	9.6	1.7	119	53
pMC1-*o*-C2Ci	1:0	7.0	1.9	35	77
pMC1-*o*-C2Ci (1:4)	1:4.1	5.0	1.5	110	44
pM-*o*-Ci	1:0	11.0	3.1	110	53
pM-*m*-Ci	1:0	13.2	3.4	95	61
pM-*p*-Ci	1:0	16.6	3.3	125	60

[a] The degree of esterification.

The following monomers were prepared in the same way:

Methyl (*E*)-2-(methacryloyloxy)-4-methoxycinnamate as colorless needles of mp 74–75 °C in 68% yield. ^{1}H-NMR ($CDCl_3$): δ (ppm) 2.00 (s, 3H, CH_3), 3.70 (s, 3H, $COOCH_3$), 5.70 (d, 1H, C=CH), 6.30 (d, 1H, C=CH), 6.38 (d, 1H, CH=C*H*COO, J = 16.7 Hz), 7.08 (d, 2H, Ar-H, J = 7.7 Hz), 7.48 (d, 2H, Ar-H, J = 7.7 Hz), 7.63 (d, 1H, C*H*=CHCOO, J = 16.7 Hz). Calcd for $C_{14}H_{14}O_4$: C, 68.30; H, 5.70. Found: C, 67.74; H, 5.69.

Methyl (*E*)-3-methacryloyloxy-4-methoxycinnamate as colorless needles of mp 42–44 °C in 36% yield. ^{1}H-NMR ($CDCl_3$): δ (ppm) 2.00 (s, 3H, CH_3), 3.75 (s, 3H, $COOCH_3$), 5.75 (d, 1H, C=CH), 6.30 (d, 1H, C=CH), (d, 1H, CH=C*H*COO, J = 16.5 Hz), 7.25 (m, 4H, Ar-H), 7.60 (d, 1H, C*H*=CHCOO, J = 16.5 Hz). Calcd for $C_{14}H_{14}O_4$: C, 68.30; H, 5.70. Found: C, 68.21; H, 5.83.

Methyl (*E*)-4-methacryloyloxy-4-methoxycinnamate as colorless needles of mp 61–62 °C in 84% yield. ^{1}H-NMR ($CDCl_3$): δ (ppm) 2.05 (s, 3H, CH_3), 3.75 (s, 3H, $COOCH_3$), 5.75 (d, 1H, C=CH), 6.43 (d, 1H, CH=C*H*COO, J = 16.5 Hz), 6.45 (d, 1H, C=CH), 7.30 (m, 4H, Ar-H), 7.73 (d, 1H, C*H*=CHCOO, J = 16.5 Hz). Calcd for $C_{14}H_{14}O_4$: C, 68.30; H, 5.70. Found: C, 68.03; H, 5.66.

Methyl (*E*)-4-methoxy-2-(2-(methacryloyloxy)ethoxy)-cinnamate as colorless needles of mp 56–57 °C in 88% yield. ^{1}H-NMR ($CDCl_3$): δ(ppm) 2.00 (s, 3H, CH_3), 3.77 (s, 3H, CH_3O), 3.82 (s, 3H, $COOCH_3$), 4.30 (t, 2H, CH_2), 5.15 (t, 2H, CH_2), 5.60 (d, 1H, C=CH), 6.10 (d, 1H, CH_2), 6.50 (m, 3H, CH=C*H*COO, J = 16.8 Hz, + Ar-H), 6.70 (m, 2H, Ar-H), 7.40 (d, 1H, Ar-H), 7.90 (d, 1H, C*H*=CHCOO, J = 16.8 Hz). Calcd for $C_{17}H_{20}O_6$: C, 63.80; H, 6.20. Found: C, 64.00; H, 6.40.

Polymerization. Azobisisobutyronitrile (AIBN) was recrystallized from methanol. A benzene solution of 10 wt % of monomers and 0.5 wt % of AIBN was placed in a tube to be degassed through freeze/thaw cycles and sealed, followed by shaking at 60–65 °C for 6 h. Precipitation of polymers (**1**–**8**) in methanol was repeated until no monomer was detected with gel permeation chromatography. Cinnamate polymers were finally dried in vacuo at room temperature. Copolymerzation ratios were estimated by UV absorption spectra of copolymers with methyl methacrylate using absorption coefficients of cinnamate model compounds. Polymers are summarized in Table 2.

Physical Measurements. Thermal properties of polymers were analyzed at a heating rate of 10 °C/min with a DSC 200 of Seiko Electronics Industry. GPC measurement was performed using a JASCO Intelligent UV detector. UV absorption spectra were taken on a Hewlett-Packard 8452 A diode array spectrophotometer or a Hitachi 320 spectrometer. Polarized absorption spectra of polymer films were recorded on the diode array spectrophotometer using a polarizer.

Photoirradiation Experiments. Light of 313 nm wavelength was obtained by passing light from a 500 W high-pressure mercury arc through a cell filled with an aqueous solution of potassium chromate and a UV D35 glass filter (Toshiba) for irradiation of polymer thin films. UV irradiation at 313 nm light for solution photochemistry was made using a JASCO spectroirradiator (CRM-FA) equipped with a xenon lamp for solution photochemistry.

Spectral Analysis. Thin films of cinnamate polymers were illuminated with 313 nm light and subjected to UV spectrum measurement at intervals. Spectral alteration was analyzed to obtain photoproduct distribution by the procedure given by Reiser et al. according to the following equations:

$$E\text{-isomer } f_E = \epsilon_E/(\epsilon_E - \epsilon_Z)[D_{\max}/D°_{\max} - (\epsilon_Z/\epsilon_E)(D_{\mathrm{iso}}/D°_{\mathrm{iso}})]$$

$$Z\text{-isomer } f_Z = \epsilon_E/(\epsilon_E - \epsilon_Z)[D_{\mathrm{iso}}/D°_{\mathrm{iso}} - (\epsilon_Z/\epsilon_E)(D_{\max}/D°_{\max})]$$

$$\text{photodimer } f_{\mathrm{dimer}} = 1 - (D_{\mathrm{iso}}/D°_{\mathrm{iso}})$$

where ϵ_E and ϵ_Z are molar extinction coefficients of the *E*- and *Z*-isomers at $\lambda_{\max}$ of the *E*-isomer of the corresponding low-mass model compound, respectively. D_{iso} and $D_{\max}$ are the absorbances during photoreaction at a wavelength of an isosbestic point for the photoisomerization and at the absorption maximum during the photoreaction, while $D°_{\mathrm{iso}}$ and $D°_{\max}$ are the corresponding absorbances before photoirradiation.[25] The molar extinction coefficient of the *Z*-isomer of cinnamates was calculated by the determination of the *E*/*Z* ratio at a photostationary state by means of HPLC analysis of the corresponding low-mass model compounds. The results are summarized in Table 1. In the case of polymers derived from methyl (*E*)-4-methoxy-2-(2-(methacryloyloxy)ethoxy)cinnamate, the photodimers absorb light of the wavelength at an isosbestic point so that *E*/*Z* ratios were obtained first according to the following expression:

$$D_{314\mathrm{nm}} = \epsilon_{E(314\mathrm{nm})}[E] + \epsilon_{Z(314\mathrm{nm})}[Z]$$

$$D_{342\mathrm{nm}} = \epsilon_{E(342\mathrm{nm})}[E] + \epsilon_{Z(342\mathrm{nm})}[Z]$$

where $D_{314\mathrm{nm}}$ and $D_{342\mathrm{nm}}$ are the absorbances at maximal wavelengths during photolysis, $\epsilon_{E(314\mathrm{nm})}$, $\epsilon_{Z(314\mathrm{nm})}$, $\epsilon_{E(342\mathrm{nm})}$, $\epsilon_{Z(342\mathrm{nm})}$ are the absorbances of *E*- and *Z*-isomers at the corresponding wavelengths, and [*E*] and [*Z*] are the concentrations of the *E*- and *Z*-isomers.

Gel Point Determination. A solution of a 1.5 wt % cinnamate polymer in a 1:1 mixed solvent of dichloromethane and chlorobenzene was spin-cast on a silicone wafer at 500 rpm for 30 s, followed by heating at 100 °C for 10 min to prepare a photo-cross-linkable film of 0.13–0.18 μm thickness. The film was exposed to light from a 200W Hg–Xe lamp (San-ei Electric Super Cure-202S) passed through a potassium chromate and a UV D35 filter (Toshiba) to select 313 nm light, subsequently treated in a mixed solvent of methyl ethyl ketone and 2-propanol for 1 min, and rinsed in 2-propanol. Film thickness was measured using a DEKTAK3ST of Japan Vacuum Technology Co.

Polarized Photoirradiation. A polymer film spin-cast on a quartz plate was irradiated with a 500 W superhigh-pressure Hg lamp through a combination of filters and a polarizer to obtain linearly polarized 313 nm light. Polarized absorption spectra was recorded on the diode array spectrophotometer equipped with a Glan-Thomson prism.

Photoalignment Regulation. A rectangular glass plate (1×3 cm^2) was spin-cast with a cinnamate polymer and irradiated with linearly polarized 313 nm light of a polarization plane angle θ, which is defined as an angle contained by a longer axis of the plate and the electric vector of the actinic light. A hybrid cell was assembled using a glass plate covered with the photoirradiated cinnamate polymer film and a lecithin-treated glass plate and filled with 4′-pentyl-4-cyanobiphenyl (5CB; $T_{\mathrm{NI}} = 35.4$ °C) according to a capillary method. The birefringence determination of the cell was carried out according to our previous papers[8–13] by passing a linearly polarized probing He–Ne laser beam through the cell and a crossed polarizer as a function of rotational angle ϕ, which is an angle between the longer axis of the plate and the electric vector of the laser beam. A 1 wt % dichroic aminoanthraquinone dye (LCD118; Merck) in 5CB was used for the evaluation of LC alignment direction.

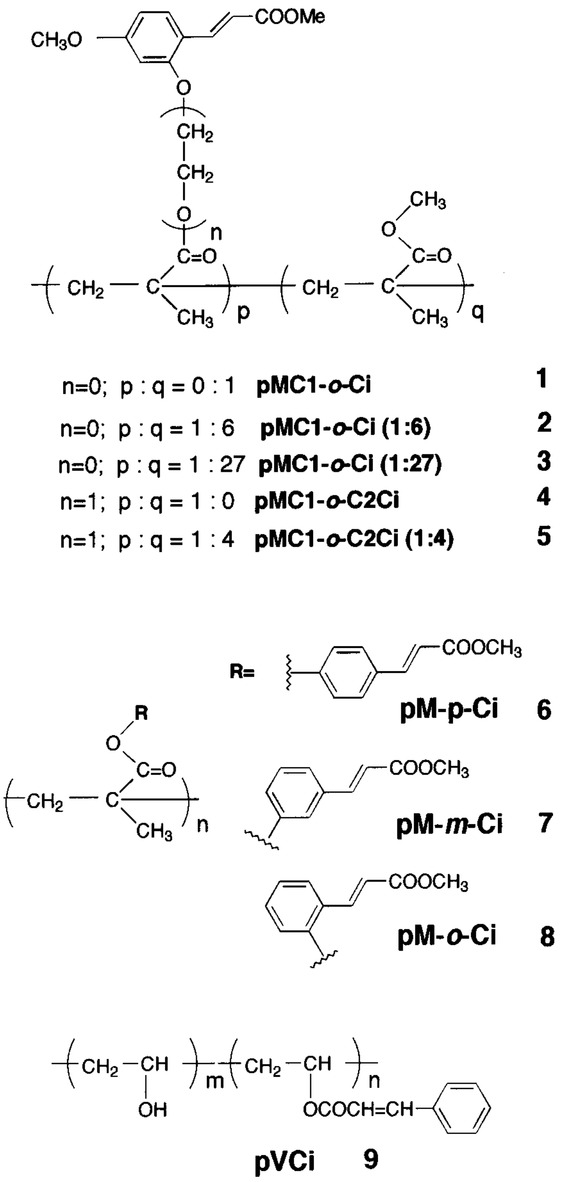

Figure 2. The structures and abbreviation of cinnamate polymers.

Results

Photochemistry in Solutions and in Films. Cinnamates polymers employed here are shown in Figure 2. pVCi (**9**) was prepared by the conventional way; the level of cinnamate substitution was 40%. Polymers having methyl cinnamate side chains at the ortho-position (**1**: pMC1-*o*-Ci, and **4**, pMC1-*o*-C2Ci) and their copolymers with MMA (**2**, **3**, and **5**) were obtained by the radical polymerization of the corresponding methacylated monomers. This kind of lateral attachment of the cinnamate residue was performed on account of our previous observation that homogeneous alignment of LC takes place efficiently when azobenzene molecules are attached to a silica surface at their ortho-position. In order to demonstrate the effect of regioisomerism of the cinnamate residue as a photoactive side chain on the LC alignment, three types of polymethacrylates (**6**, pM-*o*-Ci; **7**, pM-*m*-Ci; and **8**, pM-*p*-Ci) were synthesized. Properties of the polymers are compiled in Table 2.

Photochemistry of all polymers was monitored by taking UV absorption spectra of diluted dioxane solutions which are exposed to 313 nm light. As shown in Figure 3, cinnamate residues reached to their photostationary state within exposure energy of ca. 50 mJ/cm^2. Isosbestic points were observed in the absorption spectral changes at the early stage of UV irradiation,

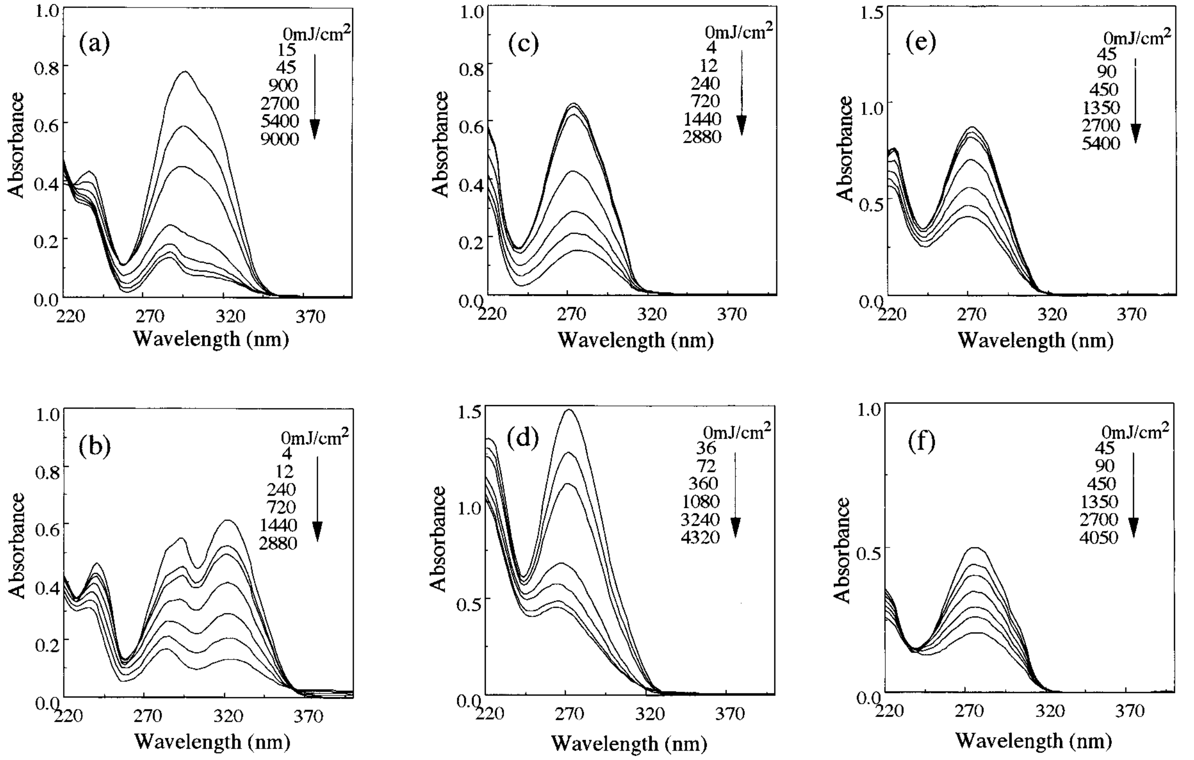

Figure 3. UV spectral change of (a) pMMe-*o*-Ci, (b) pMMe-*o*-C2Ci, (c) pVCi, (d) pM-*o*-Ci, (e) pM-*m*-Ci, and (f) pM-*p*-Ci in dioxane during the course of irradiation with 313 nm light.

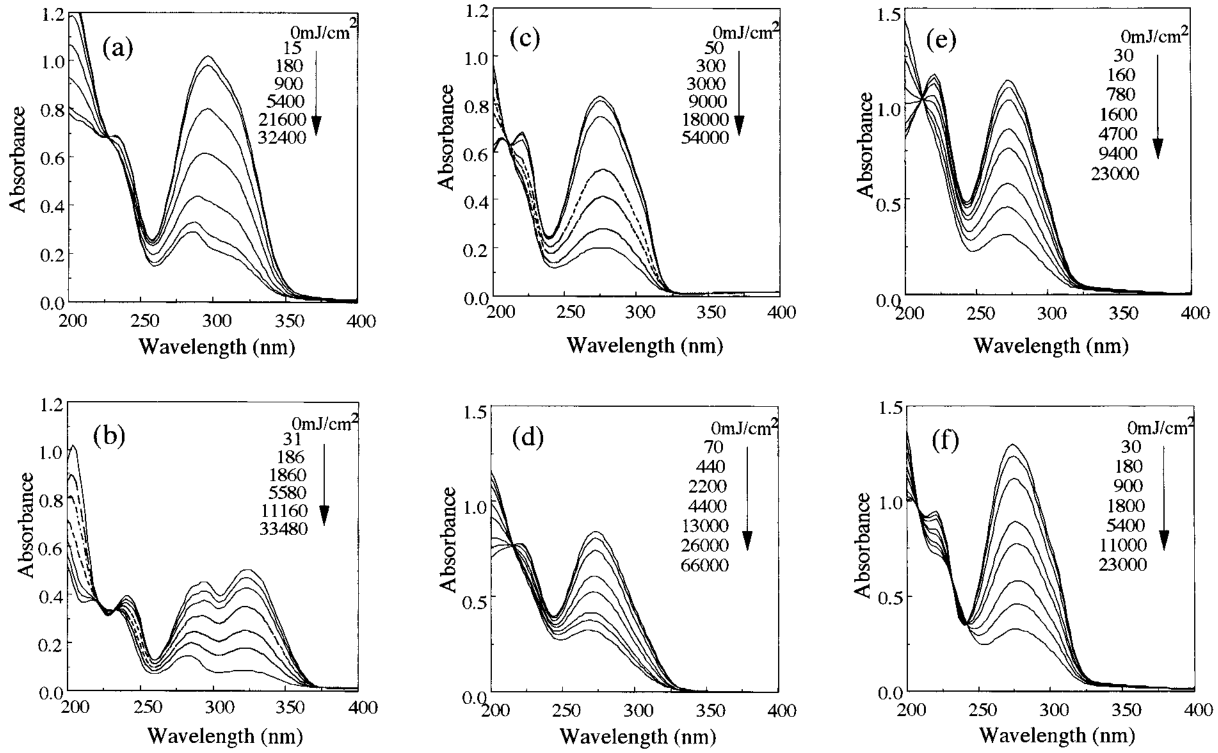

Figure 4. UV spectral change of polymer films of (a) pMC1-*o*-Ci, (b) pMC1-*o*-C2Ci, (c) pVCi, (d) pM-*o*-Ci, (e) pM-*m*-Ci, and (f) pM-*p*-Ci during the course of irradiation with 313 nm light.

as a result of exclusive *trans–cis* photoisomerization. Further photoirradiation brings about spectral changes with gradual decrease in absorbance at long absorption wavelengths, accompanied by deviation from the isosbestic points. This implies that prolonged UV irradiation leads to the photodimerization.

Spectral changes of thin films of the polymers upon UV irradiation are presented in Figure 4. Before irradiation, absorption spectra of films of all polymers coincide with those of solutions within experiment parameters; there were no difference in absorption wavelengths and half-widths of absorption band of cinnamates. These facts indicate that no alteration of spectral shape is induced by molecular interactions between cinnamate chromophores in solid films, even in the case of the homopolymer **4**. Absorption bands decrease gradually upon further irradiation with exposure energies of more than several kJ/cm^2.

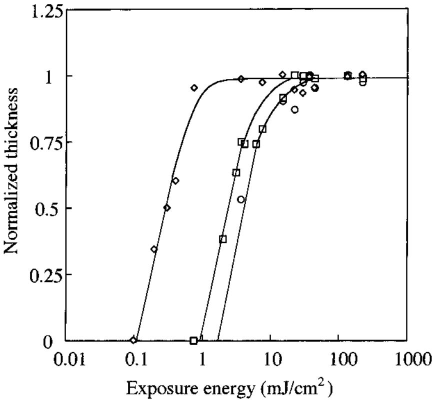

Figure 5. Insolubilization of films of pVCi (◇), pMC1-*o*-Ci (□) and pMC1-*o*-C2Ci (○) upon exposure to 313 nm light.

Photoinsolubilization. Polymers having cinnamate residues are known to be insolubilized by photoirradiation due to the 2 + 2 cycloaddition to form intermolecular cross-linkages. It was confirmed that thin films of all homopolymers presented in Table 2 became insoluble upon UV irradiation with 313 nm light. Some of the polymers prepared in this study were subjected to photogelation experiments to evaluate the photo-cross-linking efficiency. Typical examples are summarized in Figure 5. The minimum exposure energies (Eg's) for gelation of pVCi, pMC1-*o*-Ci, and pMC1-*o*-C2Ci were 0.1, 1.1, and 0.9 mJ/cm^2, respectively. Because Eg values are reversely proportional to the weight average molecular weight (M_w) of photo-cross-linkable polymers, the normalization of Eg values (Eg_{rel}) of polymethacrylates with cinnamate side chains to that of pVCi (Eg_{rel} = 1.0) was made to give 1.5 and 2.3 for pMC1-*o*-Ci and pMC1-*o*-C2Ci, respectively. The increase in the exposure energies for the latter polymers is probably due to less efficient photodimerization due to the lateral attachment of cinnamate residues.

Photoproduct Distribution in Cinnamate Polymer Films. Photoreactions of cinnamate groups in thin films as a function of exposure energy were analyzed according to Reiser's method.[25] As stated above, absorption spectra of cinnamates are not affected by film formation. This allows an accurate estimation of photoproduct distribution of cinnamate side chains with the aid of the UV absorption characteristics of the corresponding low-mass model compounds; i.e, it is assumed that absorption spectra of cinnamates tethered from polymer backbones are essentially identical with those of model compounds. Using absorption coefficients of both *E*- and *Z*-isomers of these model compounds, which are summarized in Table 1, and absorbances at the λ_{max} and an isosbestic point of the UV spectra of thin films given in Figure 3, the fractions of *E*- and *Z*-isomers and photodimers of five kinds of homopolymers were calculated as a function of exposure energy. The results, summarized in Figure 6, tell us the following: First, rates of the decrease in an *E*-isomer fraction in all polymers are reduced at early stages of photoirradiation, and even after large doses of irradiation with about 5 J/cm^2, approximately one-half of the of *E*-isomer remains unchanged. The consumption rate of the *E*-isomer is not considerably affected by the regioisomerism of the cinnamate residues. Second, the photoproduct distribution in polymer films is markedly dependent on the regioisomerism of the cinnamates. The decrease in the fraction of *E*-isomer is due to the predominant formation of *Z*-isomer formed by photoisomerization of pM-*o*-Ci, whereas the photodimerization takes place more readily for pM-*p*-Ci. The behavior of meta-isomer (pM-*m*-Ci) and the conventional photoresist (pVCi) is intermediate. Third, the photodimerizability of pM-*o*-Ci is highly suppressed when compared with that of pVCi and pM-*p*-Ci. This is due to steric hindrance induced by lateral substitution of cinnamate residues.

Polarization Photochemistry. Prolonged irradiation of a thin film of pVCi with polarized 313 nm light results in the emergence of dichroism although dichroic ratios, defined as DR = $(A_\perp - A_\parallel)/(A_\perp + A_\parallel)$, are 0.04 or less. Here, $A_\perp$ and $A_\parallel$ are absorbances at λ_{max} of cinnamates with probing light of electric vectors perpendicular to and parallel with an electric vector of actinic polarized light, respectively. The results are presented in Figure 7. Thin films of the polymethacrylates with cinnamate side chains show also photodichroism upon polarized irradiation with 313 nm light though DR values are also very small. All polymers show positive DR values, indicating that polarized light induces perpendicular reorientation of cinnamates irrespective of their regioisomerism and of their attachment modes.

The patterns of emergence of the dichroism as a function of irradiation energy are markedly dependent upon the structure of polymers and are classified into three groups. The first involves PVCi, pM-*p*-Ci, and pM-*m*-Ci, which displayed a linear increase in the DR values with the increase in exposure energy of polarized light. In the cases of pMC1-*o*-2Ci, pMC1-*o*-2Ci (1:4), and pM-*o*-Ci, belonging to the second group, an abrupt increase in the dichroism was observed at an early stage of polarized photoirradiation, followed by the decrease and the final saturation of DR upon prolonged photoirradiation. Peculiar behavior in polarization photochemistry was observed for a pM-*o*-Ci film, which demonstrated a maximum value at an exposure energy of about 50 mJ/cm^2, followed by the decrease in the value to give a constant DR. The third group containing pMC1-*o*-Ci and its copolymer showed maximum DR values, followed by the decrease, though the maximum appears more slowly than in the case of the second group.

Photoalignment Regulation of a Nematic Liquid Crystal. Alignment regulation of a nematic LC (5CB) was determined by fabricating an LC cell using a lecithin-treated silica plate and a silica plate covered with a cinnamate polymer film which is exposed to polarized 313 nm light in advance with variant exposure energies. Homogeneous alignment was monitored by measuring transmitted light intensity of a polarized He−Ne laser beam as a probing light passed through a cell and a crossed polarizer as a function of a rotational angle of the cell around an experimental optical axis. The transmitted light intensity (I/I_0) through a birefringent layer is expressed as follows:

$$I/I_0 = \sin^2(2\beta)\,\sin^2(\pi d\Delta n(\alpha)/\lambda)$$

where β is the angle between electric vectors of actinic and probing polarized light, while d, $\Delta n(\alpha)$, and λ stand for layer thickness, birefringence of an LC at a tilt angle α, and the wavelength of the probe light. Because d and λ are constant, I/I_0 is influenced directly by a tilt angle (an angle contained by the molecular axis and a substrate surface) of the LC. The results for pMC1-*o*-C2Ci and pVCi are given in Figure 8 for the representative examples. In the figure, three birefringence curves

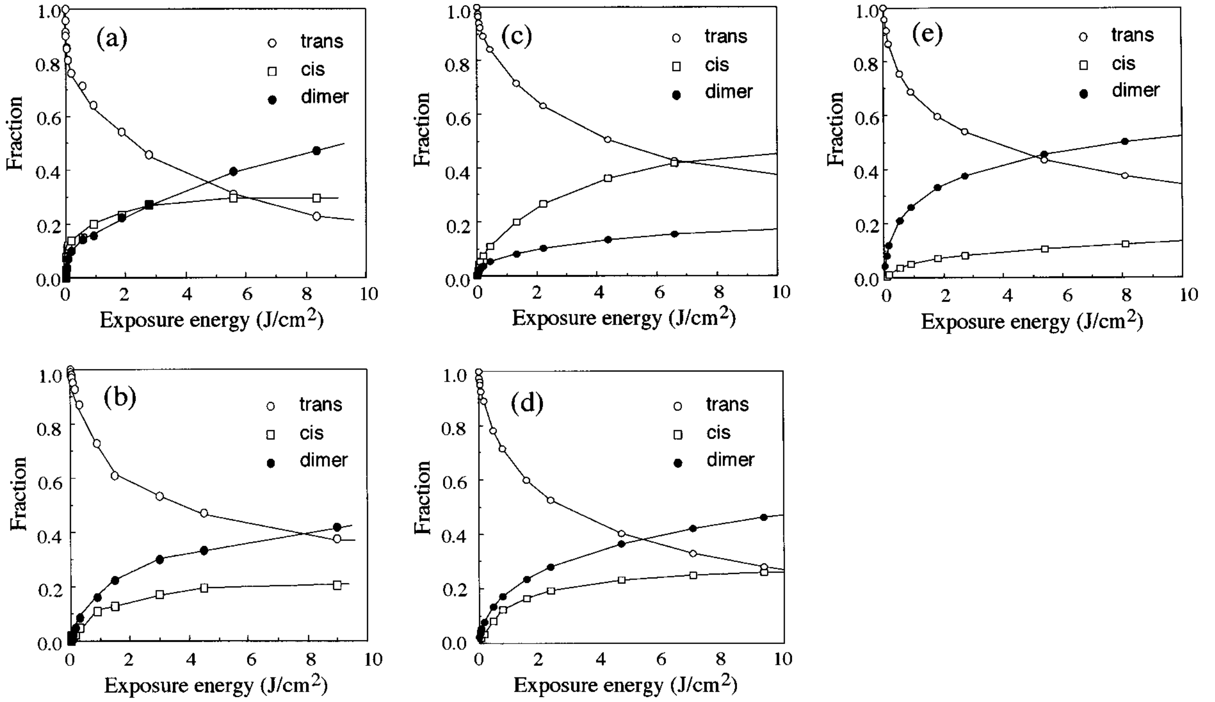

Figure 6. Fractions of *E*- (○) and *Z*- (□) isomers and photodimers (●) in thin films as a function of exposure energy for (a) pMC1-*o*-C2Ci, (b) pVCi, (c) pM-*o*-Ci, (d) pM-*p*-Ci, (e) pM-*p*-Ci.

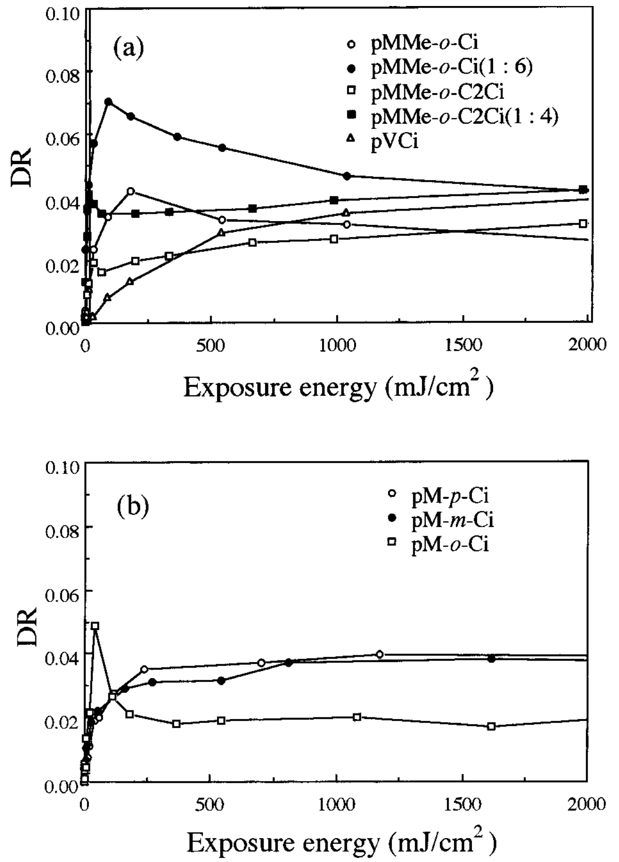

Figure 7. Dichroic ratios of films of (a) pMC1-*o*-Ci (○), pMC1-*o*-Ci (1:6) (●), pMC1-*o*-C2Ci (□), pMC1-*o*-C2Ci (1:4) (■), and pVCi(△) and of (b) pM-p-Ci (○), pM-m-Ci (●) and pM-*o*-Ci (□) as a function of exposure energy of linearly polarized 313 nm light.

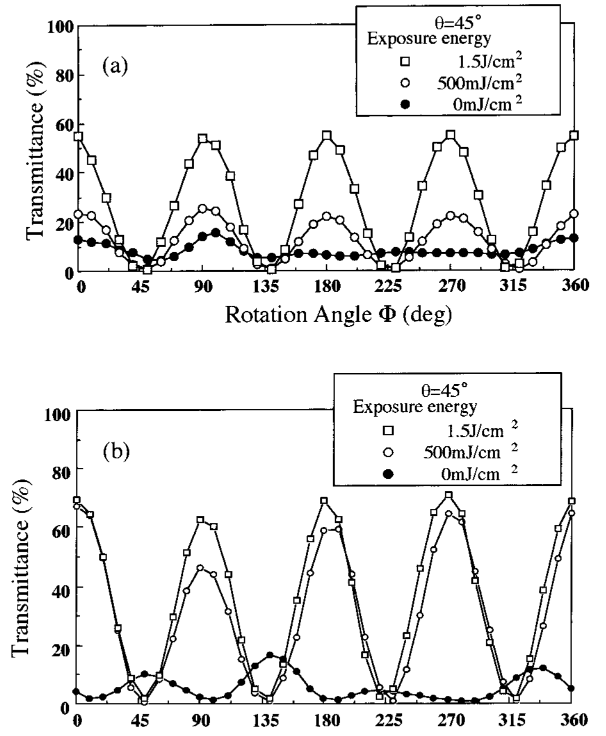

Figure 8. Angular dependence of transmitted light intensity of a monitoring linearly polarized He−Ne laser beam through LC cells covered with (a) pMC1-*o*-C2Ci and (b) pVCi, respectively. Films of pMC1-*o*-C2Ci and pVCi on silica substrate plates were irradiated with linearly polarized 313 nm light of a polarization plane angle $\theta = 45°$ with exposure energies of 0 J/cm^2 (●), 0.5 J/cm^2 (○), and 1.5 J/cm^2 (□), respectively, before cell assembly.

are presented: before, in the midst, and after polarized light irradiation giving birth to saturated birefringence. Other cinnamates polymers gave similar results. Despite the small photodichroism of cinnamate polymer thin films as shown in Figure 7, all of the polarized light irradiated films induced homogeneous alignment. The emergence of homogeneous alignment is affected considerably by the nature of cinnamate polymers. As summarized in Table 3, copolymers require a much larger exposure energy to reach a saturated alignment

Table 3. Exposure Energies of 313 nm Light Required for Homogeneous Alignment

polymers	Approximate Exposure Energy (J/cm^2)	polymers	Approximate Exposure Energy (J/cm^2)
pVCi	1.5	pMC1-*o*-C2Ci (1:4)	5.0
pMC1-*o*-Ci	1.5	pM-*o*-Ci	0.05
pMC1-*o*-Ci (1:6)	5.0	pM-*m*-Ci	0.05
pMC1-*o*-C2Ci	1.5	pM-*p*-Ci	0.05

than the corresponding homopolymers. Interestingly, the exposure energy is considerably reduced for homogeneous alignment when films of polymethacrylates with cinnamate side chain are used.

The photoinduced alignment direction was determined by measuring the dichroism of a dichroic dye dissolved in a nematic LC (5CB). The results are shown in Figure 9. It is confirmed that the alignment direction is perpendicular to an electric vector of polarized actinic light. Since the absorbance of the dichroic dye molecules is a function of a tilt angle of the dye, Figure 9 gives us information about the tilt angles. Thus, LC molecules align homogeneously by the action of a photoirradiated pM-*p*-Ci film with relatively a large tilt angle.

The thermal stability of the homogeneous alignment generated by polarized light irradiated films of cinnamate polymers was also influenced by the structure of the cinnamate polymers. The alignment induced by polarized light of an exposure energy of 1.5 J/cm^2 was completely deteriorated by heating of a cell coated with pM-*o*-Ci at 60 °C above T_{NI} for 10 min to give a schlieren texture. This is in sharp contrast to the fact that the homogeneous alignment is maintained even after heating at 120 °C for 10 min when a substrate surface is coated with the cinnamate polymers (pM-*m*-Ci, pM-*p*-Ci and pVCi) exhibiting efficient photodimerization, although disclination lines are generated, reflecting the reduction of anchoring strength. It is assumed that the intermolecular cross-linkage due to the photodimerization enhances the alignment stability owing to the suppression of the thermal randomization of the photoinduced oriented state of the chromophores.

Discussion

Photochemistry in Thin Films. Cinnamates have been widely employed as photo-cross-linkable units leading polymer backbones to insolubilization. It should be noticed that the insolubilization of a film of a cinnamate polymer like PVCi is caused by exposure to a total energy of only a few mJ/cm^2 (Figure 5). According to Charlesby's gelation theory, insolubilization takes place even when one cross-linkage is formed between two polymer chains, and the cross-linkage number of, for example, ten of linear polymers causes efficient insolubilization.[25] In other words, the photodimerization of only one percent or less of cinnamate residues of polymerization degree = 1400 of pVCi brings about the photofunctionality of pVCi as a negative-working photoresist. It is worthy of note that the photofunctionality of cinnamate polymers as negative-working photoresists emerges even though fractions of photodimers shown in Figure 6 are about 0.01 or less so that small exposure energies are needed for this purpose. On the contrary, the photoregulation of LC alignment induced by polarized light requires 3 orders of magnitude larger exposure energies, except for the polymethacrylates having regioisomeric methyl cinnamate residues (Table 3). This means that the photoinduced molecular reorientation of cinnamate residues in thin films does not result from photodimerization leading to insolubilization, at least at the early stage of the solid state photochemistry.

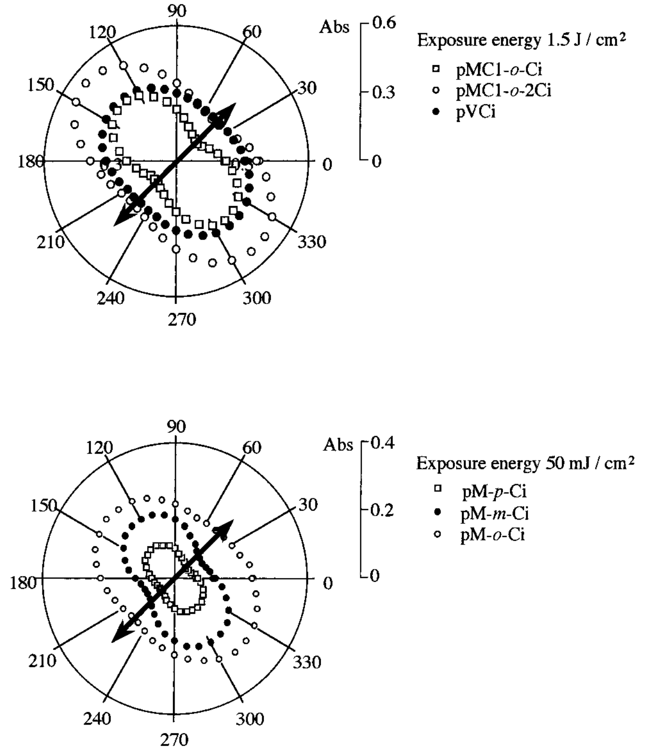

Figure 9. Polar diagrams of absorbances at 633 nm of cells filled with 5CB containing a dichroic dye. The cells were fabricated with silica plates coated with cinnamate polymer films which were exposed to linearly polarized 313 nm light in advance. (a) Exposure energy = 1.5 J/cm^2. □, pMC1-*o*-Ci, ○, pMC1-*o*-C2Ci; ●: pVCi. (b) Exposure energy = 50 mJ/cm^2. □, pM-*p*-Ci; ●: pM-*m*-Ci; ○, pM-*o*-Ci. The arrows correspond to the electric vector of actinic light.

A notable effect of the regioisomerism of cinnamate residues was observed on the photodimerization in solid films (Figure 6). In the cases of polymethacrylates with methyl cinnamate side chains, the rate of photodimerization increases in the following order: pM-*p*-Ci > pM-*m*-Ci ≫ pM-*o*-Ci. pM-*o*-Ci displays anomalously low photodimerizability among the polymers studies here. It was suggested that the intermacromolecular photodimerization of pVCi proceeds owing to its comb-like conformation, enabling the formation of an interdigitating structure of cinnamate side chains. In order to obtain information about the conformational difference between pM-*p*-Ci and pM-*o*-Ci, structural simulation was carried out using MOPAC PM3. The results visualized clearly that the cinnamate residues of pM-*p*-Ci extend out from the polymer backbone to form a comb-like conformation whereas the polymer chains of pM-*o*-Ci are disordered owing to overcrowded ortho-substitution of cinnamate residues. The distorted conformation due to ortho-substitution results in the suppression of photodimerization. It is noteworthy to mention here that pMC1-*o*-C2Ci, in which methyl *p*-methoxycinnamate residues are tethered to polymer backbones at the *ortho*-position, demonstrates a photodimerizability not much different from that of pVCi and pM-*p*-Ci. This enhanced photoreactivity of *o*-cinnamate residues may arise from the flexible ethylene spacer.

As pointed out above, photoinduced dichroism of cinnamates in polymer films is not always generated in a linear manner. A representative example is the case of polymers with side-on type cinnamate residues such as pM-*o*-Ci (Figure 7). The photodichroism emerges over a maximum. This can be reasonably interpreted as a combination of two kinds of linearly polarized light induced photochemical reactions: axial-selective destructive photochemistry and molecular reorientation due to repeated axial-selective photoisomerization.[13,26] The former process proceeds as a result of one-way photochemistry of cinnamates which are converted into *Z*-isomer preferentially when a transition moment of the chromophore is in parallel with an electric vector of polarized actinic light. This results in the axial-selective consumption of *E*-isomer to bring about optical anisotropy without any molecular reorientation. Because this type of axial-selective photochemistry is a transient event, further photoirradiation causes the photoisomerization of chromophores with a transition moment which does not lie in parallel with the electric vector of actinic light. This leads to the gradual reduction of dichroism. On the other hand, the latter molecular reorientation is caused by the axial-selective photoisomerization of both *E*- and *Z*-isomers and reaches a constant dichroic ratio after sufficient polarized photoirradiation. It should be noticed here that the maximum values of DR appear at exposure energies of less than 50 mJ/cm^2 for the side-on type cinnamate polymers. At such low exposure energies, the fraction of photodimers is so negligibly small that photodimerization plays no role in the emergence of photodichroism. The fraction of *Z*-isomers is also tiny, suggesting that there is practically no chance of undergoing molecular reorientation, which requires axial-selective photon absorption by the photoconverted *Z*-isomer. This consideration leads us reasonably to the conclusion that the abrupt increase in DR at the early stage of polarized irradiation is due to the axial-selective, destructive photoisomerization from *E*- to *Z*-isomer, followed by the gradual molecular reorientation of the chromophores. In our previous work, a quite similar phenomenon was observed for polymethacrylates with side-on type azobenzene side chains. When a thin film of a novel azobenzene polymer is irradiated with polarized blue light into the n,π*-absorption band, a DR maximum is attained with an exposure energy of *ca*. 50 mJ/cm^2, followed by a slight decrease in DR values to give a saturated value upon prolonged photoirradiation.

Such an appearance of a DR maximum seems to be characteristic of the side-on type of photoisomerizable chromophores. It is very likely that this circumstance arises from a lateral attachment of photochromic units. As mentioned in the conformational simulation of pM-*p*-Ci and pM-*o*-Ci, the latter polymer displays a rather distorted conformation to make available local free volume and allow photoisomerization. On the other hand, *p*-cinnamate side chains of the former polymer seem to be of an interdigitating structure, which minimizes free volume and suppresses photoisomerization.

It should be mentioned here that the DR maximum appears at larger exposure energies (a few hundred mJ/cm^2) for pMC1-*o*-Ci and its copolymer when compared with the other side-on type cinnamate polymers (pM-*o*-Ci and pMC1-*o*-C2Ci). The structural difference between pM-*o*-Ci and pMC1-*o*-Ci exists solely on where the *p*-methoxy residue is substituted on the benzene ring. In other words, a methoxy group influences the photoisomerizability in solid films probably due to the increase in sweep volume. pMC1-*o*-C2Ci bears the same *p*-methoxy cinnamate residue through a ethylene spacer. The difference in the generation of photodichroism between pMC1-*o*-Ci and pMC1-*o*-C2Ci arises therefore from the spacer.

As shown in Figure 3, a photostationary state is obtained upon 313 nm light irradiation of a solution of a cinnamate polymer with exposure energy of less than 50 mJ/cm^2, and photodimerization takes place subsequently. In a direct contrast to this, as Figure 6 tells us, there is no photostationary state in the solid state, and *E*/*Z* photoisomerization proceeds with a considerably low rate for all polymers. The photoisomerization of cinnamates in films occurs much more slowly than that of azobenzenes. The suppression of the photoisomerization of cinnamates in the solid state may be ascribable to the C═C double bond, which isomerizes inevitably through the rotational mechanism, while azobenzenes have a chance to isomerize via the inversion mechanism requiring a smaller sweep volume. The rotation of partial residues of cinnamates, the methoxycarbonyl residue, needs a significantly larger free volume to have a suppressive effect on the isomerization in polymer solids.

Photoalignment Mechanism. Figures 6 and 7 give us further insight into the mechanism of LC photoalignment induced by cinnamate polymer films. Note first that the polymethacrylates attached with cinnamates at the benzene ring (pM-*o*-Ci, pM-*m*-Ci, and pM-*p*-Ci) require exposure energies of about 50 mJ/cm^2 while more than 1 order of magnitude greater energy is needed to obtain a homogeneous alignment when pVCi is employed (Table 3). As seen in Figure 6, the fractions of photodimers are negligibly small in films of the poly(methacrylates) with such a low exposure energy (50 mJ/cm^2), indicating that the LPL-induced photodimerization plays practically no role in the photoalignment regulation. This observation suggests unequivocally that the *E*/*Z* photoisomerization plays a role in the alignment photoregulation induced by cinnamate polymers. The role of the photoisomerization in the photoalignment was additionally disclosed by the following experiment. A half area of a polymer film spin-cast on a silica plate was first irradiated with polarized 313 nm light of an energy of 3.0 J/cm^2 to lead to a homogeneous alignment. Subsequently, the whole area was illuminated with 313 nm light after rotating the polarization plane of actinic light by 45°, followed by a cell assembly to observe LC textures using a polarized microscope. The results were remarkable. A uniformly homogeneous alignment was observed in the whole area for a cell coated with pM-*o*-Ci, showing that the reorientation of LC is generated completely by the second exposure. This shows that the photoalignment is caused by polarized photoisomerization of the cinnamate residues, because no photon can be absorbed by the photodimers. Contrary to this, when the substrate surface was coated with films of pM-*m*-Ci, pM-*p*-Ci, and pVCi, respectively, the homogeneous alignment induced by the first LPL irradiation was memorized so that no reorientation was complete after the second LPL irradiation of LC cells. As shown in Figure 6, after irradiation with UV light with an exposure energy of 3 J/cm^2, the fraction of photodimers of pM-*o*-Ci amounts to around 10%, whereas those of pM-*m*-Ci, pM-*p*-Ci, and pVCi are approximately 30%, 38%, and 30%, respectively. It is reasonable to conclude that the sufficient LC alignment reorientation in a cell coated with pM-*o*-Ci is owing to the polarized *E*/*Z* photoisomerization, leading to the molecular reorientation of the cinnamate residues, as in the case of azobenzenes.[12,13]

As stated above, the homogeneous alignment induced by a polarized light irradiated film of pM-*o*-Ci disappears completely after heat treatment above T_{NI}, whereas a uniaxially aligned texture was maintained more or less when a cell is assembled with a plate coated with a film of the other cinnamate polymers. There is a clear difference in the photochemical behavior between pM-*o*-Ci and the other polymers. The fraction of photodimers is quite small (ca. 10%) for pM-*o*-Ci, as described above. The lower density of cross-linkage cannot suppress sufficiently the thermal randomization of photooriented cinnamate residues. This means that the photodimerization plays a key role in the thermal stabilization of photoinduced LC alignment.

Conclusion

Photoproduct distribution in thin films of polymers with cinnamate side chains is markedly dependent on the regioisomerism of the chromophores. UV irradiation of a film of a polymethacrylate (pM-*o*-Ci) with *ortho*-cinnamate residues results predominantly in the geometrical E-to-Z photoisomerization, accompanied by dimerization as a minor photoprocess, while the latter takes place more favorably when films of pM-*p*-Ci and pVCi are subjected to UV illumination. Peculiar behavior of pM-*o*-Ci was again observed in the polarization photochemistry of its thin film. All polymers having cinnamate residues possess the photocontrollability to give a homogeneous LC alignment upon polarized UV irradiation. It has been concluded that the photoalignment of LC molecules is induced not by the axially selective photodimerization, but by the polarized E/Z photoisomerization of cinnamate chromophores, just as in the case of azobenzene polymers. Photodimerization contributes to the enhancement of thermal stability of LC photoalignment because of the suppressive effect of the cross-linked structure on the randomization of photochemically oriented chromophoric residues. Thin films of cinnamate polymers offer specific command surfaces with thermal stability.

Acknowledgment. This work was supported by a Grant-in-Aid on Priority-Area-Research “Photoreaction Dynamics” from the Ministry of Education, Sport, Science and Culture (K.I.) and by a Grant from NEDO (New Energy Development Organization) (K.I.). We thank Dr. John Sperry for his help with the manuscript preparation.

References and Notes

(1) Minsk, L. M.; Smith, J. G.; Van Deusen, W. P.; Wright, J. F. *J. Appl. Polym. Sci.* **1959**, *2*, 302.
(2) Kvasnikov, E. D.; Kozenkov, V. M.; Barachevsky, V. A. *Zh. Nauchn. Prikl. Fotogr. Kinematogr.* **1979**, *24*, 222; *Chem. Abstr.* **1979**, *91*, 99887*h*.
(3) Barachevsky, V. A. *SPIE* **1991**, *1559*, 184.
(4) Gibbons, W. M.; Shannon, P. J.; Sun, S.-T.; Swetlin, B. J. *Nature* **1991**, *351*, 49.
(5) Shannon, P. J.; Gibbons, W. M. Sun, S.-T. *Nature* **1994**, *368*, 532.
(6) Gibbons, W. M.; Shannon, P. J.; Sun, S.-T. *Mol. Cryst. Liq. Cryst.* **1994**, *251*, 191.
(7) Iimura, Y.; Kusano, J.; Kobayashi, S.; Aoyagi, T.; Sugano, T. *Jpn. J. Appl. Phys., Part* 2 **1993**, *32*, L93.
(8) Kawanishi, Y.; Tamaki, T.; Sakuragi, M.; Seki, T.;. Suzuki, Y.; Ichimura, K. *Langmuir* **1992**, *8*, 2601.
(9) Kawanishi, Y.; Tamaki, T.; Sakuragi, M.; Seki, T.; Ichimura, K. *Mol. Cryst. Liq. Cryst.* **1992**, *218*, 153.
(10) Ichimura, K.; Hayashi, Y.; Ishizuki, N. *Chem. Lett.* **1992**, 1063.
(11) Ichimura, K.; Hayashi, Y.; Akiyama, H.; Ikeda, T.; Ishizuki, N. *Appl. Phys. Lett.* **1993**, *63*, 449.
(12) Ichimura, K.; Akiyama, H.; Ishizuki, N.; Kawanishi, Y. *Makromol. Chem., Rapid Commun.* **1993**, *14*, 813.
(13) Akiyama, H.; Kudo, K.; Ichimura, K. *Macromol. Rapid Commun.* **1995**, *16*, 35.
(14) Schadt, M.; Schmitt, K.; Kozinkov, V.; Chigrinov, V. *Jpn. J. Appl. Phys.* **1992**, *7*, 2155.
(15) Schadt, M.; Seiberle, H.; Schuster, A.; Kelly, S. M. *Jpn. J. Appl. Phys.* **1995**, *34*, L764.
(16) Schadt, M.; Seiberle, H.; Schuster, A.; Kelly, S. M. *Jpn. J. Appl. Phys.* **1995**, *34*, 3240.
(17) Dyadyusha, A. G.; Marusii, T. Y.; Reznikov, Y. A.; Khizhnyak, A. I.; Reshetnyak, V. Y. *JETP Lett.* **1992**, *56*, 17.
(18) Marusii, T. Y.; Koznikov, Y. A. *Mol. Mater.* **1993**, *3*, 161.
(19) Dyadyusha, A. G.; Khizhnyak, A.; Marusii, T. Y.; Reshetnyak, V. Y.; Reznikov, Y. A.; Park, W. S. *Jpn. J. Appl. Phys.* **1995**, *34*, L1000.
(20) Akita, Y.; Akiyama, H.; Kudo, K.; Hayashi, Y.; Ichimura, K. *J. Photopolym. Sci. Technol.* **1995**, *8*, 75.
(21) Iimura, Y.; Satoh, T.; Kobayashi, S.; *J. Photopolym. Sci. Technol.* **1995**, *8*, 257.
(22) Tomita, H.; Kudo, K.; Ichimura, K. *Liq. Cryst.* **1996**, *20*, 171.
(23) Ichimura, K.; Akita, Y.; Akiyama, H.; Hayashi, Y.; Kudo, K. *Jpn. J. Appl. Phys.* **1966**, *35*, L996.
(24) Egerton, P. L.; Pitts, E.; Reiser, A. *Macromolecules* **1981**, *14*, 95.
(25) Ichimura, K. *Makromol. Chem.* **1987**, *188*, 2973.
(26) Michl, J. *Photochromism: Molecules and Systems*, Dürr, H.; Bouas-Laurent, H., Eds.; Elsevier: Amsterdam, 1990; p 919.

MA961225Q